



Torrential rainfall with severe flooding associated with a baroclinic disturbance on November 17, 2023, United Arab Emirates (UAE)

Farahnaz Fazel-Rastgar, Masoud Rostami, Bijan Fallah & Venkataraman Sivakumar

To cite this article: Farahnaz Fazel-Rastgar, Masoud Rostami, Bijan Fallah & Venkataraman Sivakumar (11 Feb 2025): Torrential rainfall with severe flooding associated with a baroclinic disturbance on November 17, 2023, United Arab Emirates (UAE), International Journal of River Basin Management, DOI: [10.1080/15715124.2025.2462575](https://doi.org/10.1080/15715124.2025.2462575)

To link to this article: <https://doi.org/10.1080/15715124.2025.2462575>



© 2025 The Author(s). Published by Informa UK Limited, trading as Taylor & Francis Group



View supplementary material [↗](#)



Published online: 11 Feb 2025.



Submit your article to this journal [↗](#)



View related articles [↗](#)



View Crossmark data [↗](#)

Torrential rainfall with severe flooding associated with a baroclinic disturbance on November 17, 2023, United Arab Emirates (UAE)

Farahnaz Fazel-Rastgar^{a,b}, Masoud Rostami^{c,d}, Bijan Fallah^e and Venkataraman Sivakumar^b

^aSchool of Chemistry and Physics, University of KwaZulu Natal, Durban, South Africa; ^bS. V. Raman Researchers Roadmap, Westville, Durban, South Africa; ^cPotsdam Institute for Climate Impact Research (PIK), Potsdam, Germany; ^dLaboratoire de Météorologie Dynamique (LMD), Sorbonne University (SU), Ecole Normale Supérieure (ENS), Paris, France; ^eGerman Climate Computing Center (DKRZ), Hamburg, Germany

ABSTRACT

This work examines a severe weather event caused by a baroclinic disturbance with heavy rainfall and thunderstorms, which struck parts of the UAE and caused major flooding on November 17, 2023. A low-pressure trough extending from the Red Sea Trough (RST) towards the Eastern Mediterranean (EM) led to extreme flooding. The unique intensity of this heavy rainfall was correlated to mid-latitude disturbance amplification even in the middle and upper tropospheric produced by RST. During the rain event, two intense moisture sources were injected into the region: one from the Indian Ocean, carried by southeasterly near-surface winds at 10m, and the other from the Red Sea and Equatorial Africa, transported at a mid-tropospheric level. A significant temperature gradient with ~8 °C difference in surface temperatures, particularly between the northern areas in contrast with the southern regions, and the wind shear formation over the northern parts of the study area initiated the baroclinicity structure in the borderlines of the cold front and thunderstorms. The findings also revealed an abnormal westerly jet stream intensification at 200 hPa, associated with a negative meridional wind anomaly, signaling the stretching of a Rossby wave over the study area during the heavy rainfall and flooding.

ARTICLE HISTORY

Received 6 January 2025
Accepted 31 January 2025

ASSOCIATE EDITOR

Michael Nones

KEYWORDS



Baroclinic disturbance; heavy rainfall; flooding; Red Sea Trough; Rossby wave; UAE

1. Introduction

Extreme rainfall events associated with climate change are among the most threatening natural hazards, initiating widespread socio-economic disruption across the globe. Notably, arid and semi-arid regions, are subject to sporadic severe rainfall events, which can lead to flash floods with significant societal repercussions, such as substantial economic losses and loss of life (Fink and Knippertz 2003, Llasat *et al.* 2010, Almazroui 2011, Moawad 2012, De Vries *et al.* 2013, Fazel-Rastgar 2020, Fallah *et al.* 2023, Didovets *et al.* 2024, Fallah *et al.* 2024, Fallah and Rostami 2024). While much of the Middle East is classified as arid or semi-arid, characterized by limited annual precipitation, these regions occasionally experience extreme weather events that produce devastating socioeconomic impacts (Llasat *et al.* 2010, De Vries *et al.* 2013, Elsayed *et al.* 2021, Fazel-Rastgar and Sivakumar 2023).

Several parts of the Middle East, including the southeastern Mediterranean, eastern Egypt, Israel, Jordan, Lebanon, the Sinai Peninsula, Syria, and Iran, are regularly influenced by the Red Sea Trough (RST) and the Mediterranean low-pressure system (Dayan *et al.* 2001, Tsvieli and Zagvil 2007, De Vries *et al.* 2013, Rousta *et al.* 2016, Esmaeili *et al.* 2022, Insua-Costa *et al.* 2022). RST is a quasi-permanent low-level feature that is characterized by an inverted trough of low pressure at the lower troposphere continuing northward from the southern Red Sea toward the eastern Mediterranean (Ashbel 1938, El-Fandy 1948). It recognizes its largest amplitude in the lower troposphere and is greatly prompted by the topography of the surrounding region

(El-Fandy 1950, Krichak *et al.* 1997a, 1997b, Alizadeh *et al.* 2021). Red Sea Trough and the Mediterranean low-pressure system are critical drivers of precipitation in the region, often associated with the Active RST (De Vries 2013). The RST, defined as the northward extension of a southern Red Sea low-pressure system, often merges with eastern Mediterranean cyclones at lower atmospheric levels (El-Fandy 1948). Its formation is primarily driven by the development of the Sudan Monsoon Low, a large-scale subtropical-equatorial thermal low-pressure system, which typically originates near South Sudan and southeastern Sudan or along the periphery of the northern Red Sea (Awad and Almazroui 2016). The intensity and northward reach of the RST are influenced by thermal forcing and topographical conditions over the Red Sea region (Itzigsohn 1995, Krichak *et al.* 1997a, 1997b). Additionally, the system's behavior is modulated by interactions with the Siberian High and Azores High-pressure systems. When the Siberian High intensifies, the trough is deflected westward, while an intensification of the Azores High shifts it eastward (Awad and Almazroui 2016). In general, the RST is mostly active during the fall, winter, and spring, it typically dissipates during the summer due to the development of the Persian trough and localized heat lows (Kahana *et al.* 2002, Tsvieli and Zangvil 2005, De Vries *et al.* 2013, Mohammadi *et al.* 2021, Kadhun *et al.* 2022, Ziv *et al.* 2022). Overall, the following previous research highlighted the significant role of the RST and Mediterranean low-pressure systems, in causing extreme rainfall and flash floods in the Middle East. Studies show that these

CONTACT Farahnaz Fazel-Rastgar  farah_rast@yahoo.com  School of Chemistry and Physics, University of KwaZulu Natal, 4000, Durban, South Africa; S. V. Raman Researchers Roadmap, 4000, Westville, Durban, South Africa

© 2025 The Author(s). Published by Informa UK Limited, trading as Taylor & Francis Group

This is an Open Access article distributed under the terms of the Creative Commons Attribution-NonCommercial-NoDerivatives License (<http://creativecommons.org/licenses/by-nc-nd/4.0/>), which permits non-commercial re-use, distribution, and reproduction in any medium, provided the original work is properly cited, and is not altered, transformed, or built upon in any way. The terms on which this article has been published allow the posting of the Accepted Manuscript in a repository by the author(s) or with their consent.

features are key drivers of precipitation, especially in fall, winter, and spring, and their behavior is influenced by regional topography and larger atmospheric patterns like the Siberian and Azores Highs. However, climate change is linked to an increase in the frequency and intensity of these extreme weather events, leading to severe socio-economic impacts. In this study, we analyze the severe rainstorm event of November 17, 2023, in the UAE, which was characterized by intense precipitation and resulted in significant flooding.

Adverse weather in the UAE has resulted in some disruption to flights at Dubai's main airport and waterlogging on most of the main roads in the country. Also, Dubai Airshow, as a major industry was scheduled for a later time (<https://www.onmanorama.com/news/world/2023/11/17/uae-rain-dubai-flights-cancelled-schools-online-mode.html>). The UAE National Centre of Meteorology issued orange and yellow alerts nationwide, warning residents about potentially dangerous weather conditions for outdoor activities.

It is noted that during this time heavy rainfall and thunderstorms were reported across parts of the Middle East including some parts in the west, northwest, and southern areas in Iran, eastern Iraq, and Kuwait.

The specific objectives of the research are to characterize the meteorological features of the storm by analyzing the synoptic and dynamics of the severe weather event on November 17, 2023, in UAE. This work focuses on the role of RST and the Mediterranean cyclone in driving heavy rainfall and thunderstorms in the UAE. With such complex interactions, this study seems to provide new meteorological insights into the mechanisms behind severe weather in the region, which is critical for improving forecasting and preparedness. By addressing these objectives, this research can contribute to a deeper understanding of how mid-latitude disturbances and localized meteorological phenomena can combine to cause severe weather in the UAE, a region traditionally associated with arid conditions. This research not only aids in addressing regional climate risks but also may provide valuable knowledge for understanding the broader global climate, disaster management, and sustainable development in other similar arid and semi-arid regions.

2. Materials and methods

The data utilized in this study were sourced from multiple high-resolution reanalysis models and observational datasets. Specifically, the Modern-Era Retrospective Analysis for Research and Applications (MERRA) dataset from NASA was employed (Rienecker *et al.* 2011). Additionally, we analyzed ERA5 hourly data (Hersbach *et al.* 2020) provided by the ECMWF, which includes parameters such as wind speed, temperature, humidity at 850 hPa, relative vorticity at 850 hPa, and geopotential height fields at 500 hPa for the study period.

Furthermore, we incorporated meteorological datasets from the National Centers for Environmental Prediction-National Center for Atmospheric Research (NCEP-NCAR) reanalysis, which provides various atmospheric parameters. Data were analyzed using 6-hourly mean sea level pressure (SLP) records from NCEP-NCAR, available on a $2.5^\circ \times 2.5^\circ$ latitude-longitude grid (Kalnay *et al.* 1996, Kistler *et al.* 2001). Daily composite maps are created by averaging the mean values (calculated every six hours) for each grid

point. Anomalies are then calculated by subtracting the long-term mean (normal mean climatology) from these daily composites. The normal mean climatology is based on data from 1991-2020, which replaced the previous baseline of 1981-2010. This update helps reflect more recent climate patterns. The World Meteorological Organization (WMO) defines baseline reference periods for climate data to ensure consistency in comparisons and climate monitoring.

Additionally, hourly satellite imagery was retrieved from the EUMETSAT archive.

2.1. Study area and precipitation data

The climate of the United Arab Emirates (UAE) is classified as arid desert, characterized by two primary seasons—winter and summer—interspersed with two transitional periods. According to the Köppen climate classification system, this region exhibits a hot desert climate (Peel *et al.* 2007). The UAE is characterized by extreme aridity, with mean annual temperatures exceeding 18°C . Precipitation is limited and demonstrates significant temporal and spatial variability. The average annual rainfall in the UAE is approximately 78 mm, ranging from 40 mm to 125 mm in the southern desert areas, with a maximum of around 160 mm recorded in the northeastern mountainous regions (Ouarda *et al.* 2014). The UAE is also prone to violent dust storms, locally referred to as shamal winds (Yu *et al.* 2016). Figure 1a shows a world map locating UAE and Figure 1b presents a geographical map of the UAE, located in the Arabian Peninsula (source: <http://www.maps-of-the-world.net/>).

Table 1 illustrates total rainfall amounts from various weather stations across the UAE for November 2023. Data were sourced from the Federal Competitiveness and Statistics Centre (<https://fcsc.gov.ae/en-us>). It is evident from Table 1 that a maximum accumulation recorded at Dubai Airport was approximately 47 mm over three days during November 2023. However, it was reported that there was zero total accumulation during November 2022 for this weather station (<https://fcsc.gov.ae/en-us>).

Also, it is noted that the monthly total rainfall for the year 2023, highlighting that the total rainfall for November 2023 ranks as the second highest after January 2023 at Dubai Airport, totaling 89.9 mm. Based on the long-term precipitation data (1991-2020) obtained from the World (WMO) Meteorological Organization (WMO) data ("World Meteorological Organization Climate Normals for 1991-2020: Dubai Intl Airport" (XLSX). administration. p. 1. Retrieved 24 Sep. 2024) for Dubai International airport shows the wettest month in this station is January with an average of 20.8 mm of rain. However, the normal rainfall for November is 5.9mm.

To corroborate the observed heavy rainfall event on November 17, 2023, satellite imagery from EUMETSAT reveals the passage of a cloud system over the study area, coinciding with increased precipitation rates. Figure 2 (top and bottom) depict an active baroclinic leaf over the eastern Persian Gulf, extending towards the western and northern coastal areas of the UAE, with precipitation rates peaking at approximately 30 mm/hr (~5 times of normal value) during late November 16, 2023, and into the early hours of the following day. A baroclinic leaf represents a cloud system or moisture pattern typically located on the leading edge of



(a)



(b)

Figure 1. (a) A world map of the United Arab Emirates, and (b) a map of the United Arab Emirates (UAE). Source from <http://www.maps-of-the-world.net/>.

mid-tropospheric troughs, often downstream of positive potential vorticity (PV) anomalies. This pattern is associated with surface baroclinic features or cold front systems, and a mature baroclinic leaf possesses a significant potential for cyclogenesis.

3. Results and discussion

Figure 3a illustrates the mean sea level pressure (MSLP) on November 17 at 0400Z, highlighting the Arabian High-pressure system centered at 1020 hPa which is intensified at ~ 4.5 hPa rather than long-term climatology mean departure from 1991–2020 (figure is not presented here) over northern Saudi Arabia. This figure also depicts the RST with a central pressure of 1005 hPa, extending westward and southward, manifesting an isobaric pattern of approximately 1016 hPa over the study area. In contrast, the

northern and central portions of the study area exhibit a closed high-pressure isobaric pattern (~ 1020 hPa), resulting in a pronounced pressure gradient resulting in atmospheric instability predominantly in these regions. In all Figures 3–10, the x-axis represents latitude, and the y-axis represents longitude in degrees. Table 2 shows the graphical scale of the conversion of Latitude and Longitude Differences to Kilometers and Miles. This table gives a visual representation of distance on the charts presented here.

The mid-tropospheric geopotential height map (Figure 3b) at 500 hPa reveals an intense deep westerly trough over western Iran, accompanied by two minor troughs exhibiting notable gradients across the northern and western sectors of the study region. Additionally, a subtropical high-pressure system showing the mid-tropospheric ridge is evident over the lower latitudes in the Indian Ocean, extending northwest into Africa and centered over the Sudan.

Table 1. Total monthly rainfall and number of rainy days in Nov. 2023 in weather stations in UAE.

Weather Stations	Abu Dhabi Airport Station	Al Ain Airport Station	Dubai Airport Station	Sharjah Airport Station	Ajman Station	Umm Al Quwain Station	Ras Al Khaimah Airport Station	Fujairah Airport Station
Climate Indicators								
Rainfall	5.0	5.8	47.0	25.4	15.3	30.0	20.1	31.8
Rainy Days	3.0	3.0	3.0	7.0	6.0	4.0	5.0	4.0

Source: Federal Competitiveness and Statistics Centre.

The subtropical high is a high-pressure zone found around 30° latitude in both hemispheres, where air sinks from the Hadley Cells. This descending air creates clear skies, warm temperatures, and dry conditions, leading to desert climates. The Arabian Peninsula, located within this zone, experiences intense heat and very little rainfall due to this atmospheric circulation. Figure 3c presents anomaly maps (departures from the 1991–2020 climatological mean) for MSLP and 500 hPa geopotential height on

November 17, 2023. The anomalies indicate a slight intensification of both the Arabian high (+2 hPa) and the Red Sea trough (−2 hPa). Notably, geopotential height anomalies illustrate an intensification of the subtropical ridge (approximately +80 gpm) primarily over Israel and Jordan, while a deepening of −20 gpm is observed over Iran (gpm stands for geopotential meter). Furthermore, the 500 hPa geopotential height over the northern part of the study area shows a slight deepening (~5–10 gpm) compared to long-term

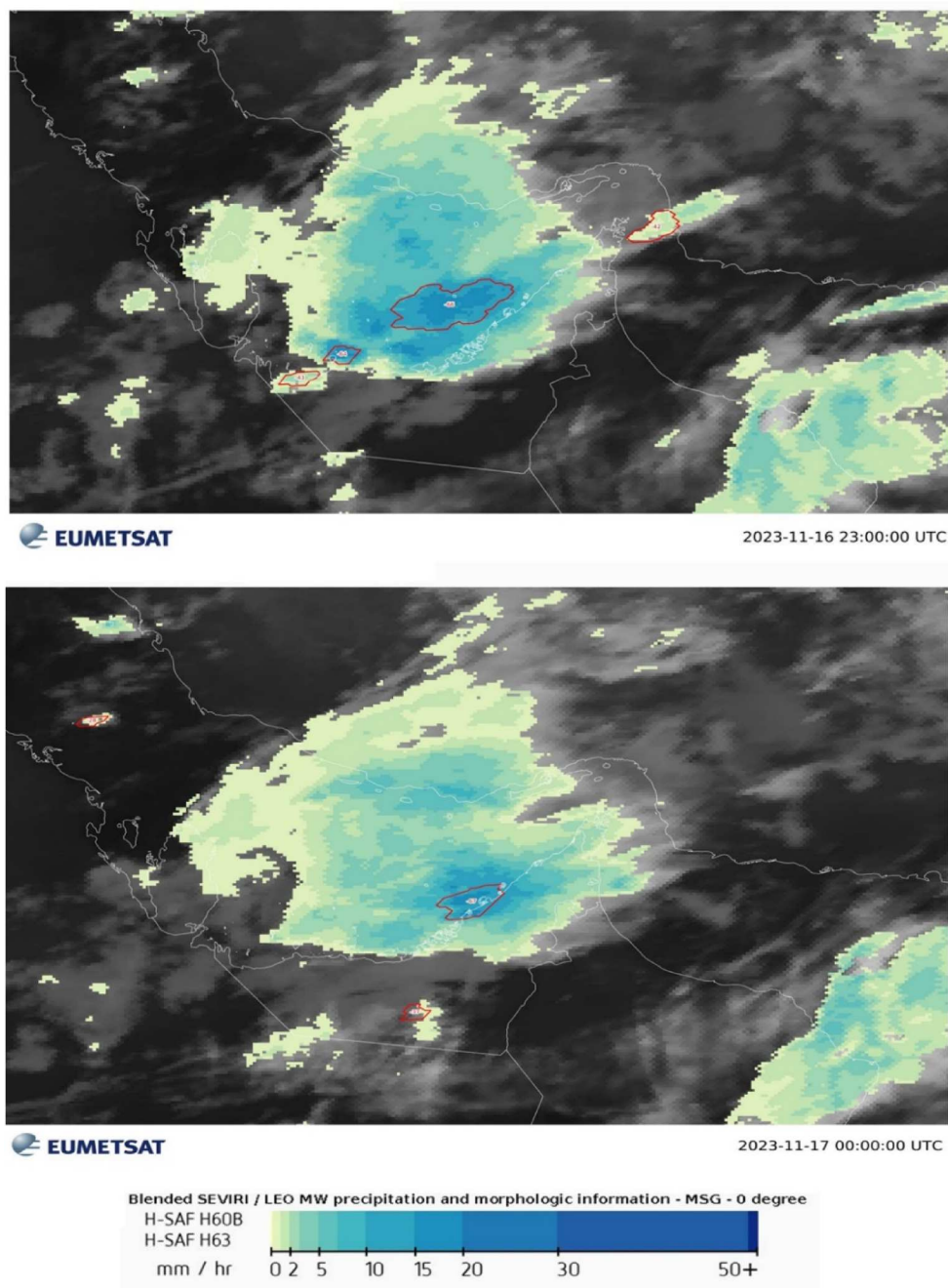


Figure 2. EUMETSAT imagery depicting ground precipitation rates on late November 16, 2023 (upper panel) and early morning on November 17, 2023 (lower panel).

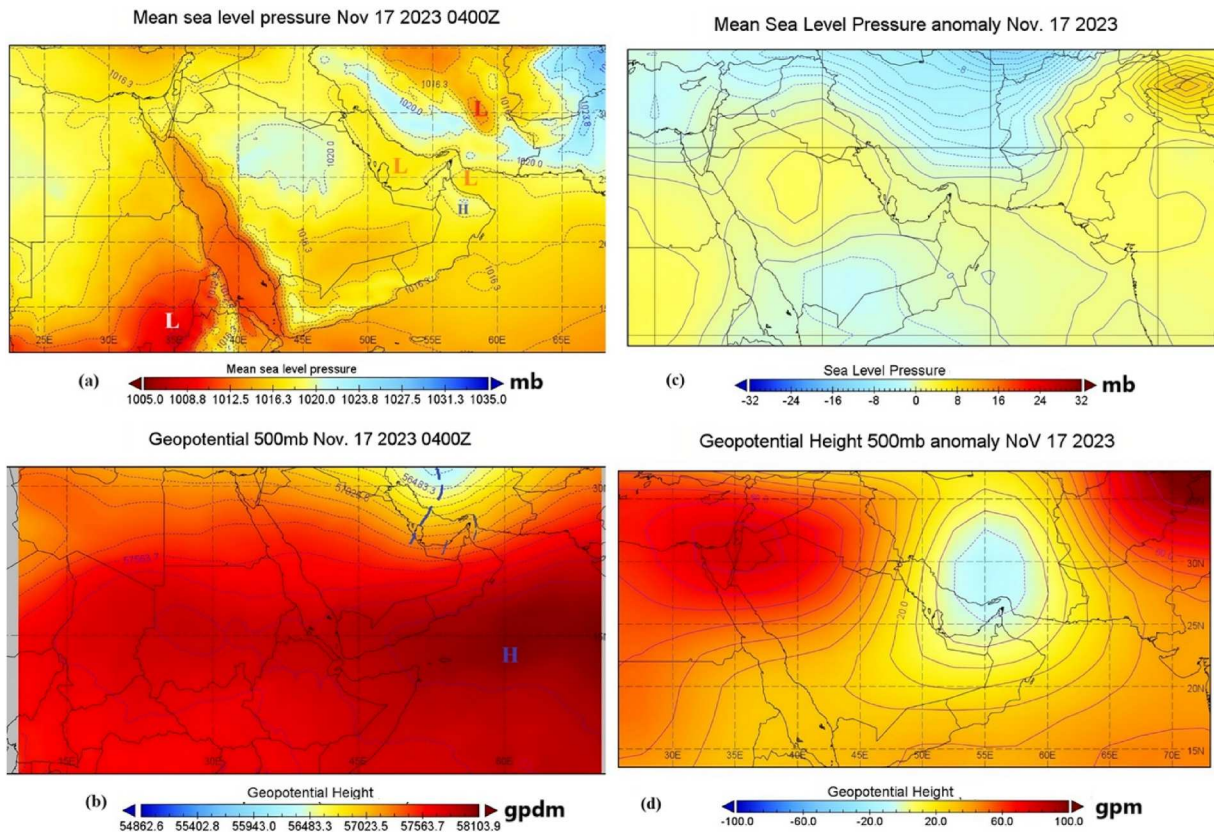


Figure 3. (a) Mean sea level pressure and (b) 500 mb geopotential height on November 17, 2023, at 0400Z. Anomaly maps showing deviations from the 1991–2020 climate averages for (c) mean sea level pressure and (d) 500 mb geopotential height over the study area on November 17, 2023. The gpm stands for geopotential decameter (gpm times ten).

climate mean values. Therefore, both [Figure 3c](#) and [Figure 3d](#) together, depict an atmospheric instability linked to the increase in the gradients of low and mid-tropospheric isolines over the study area during the extreme rainfall event.

Hourly temperature profiles at 500 hPa, shown in [Figure 4](#) for 0000Z (a), 0003Z (b), and 0004Z (c), reveal two prominent mid-tropospheric cold air troughs developing from the west and east, deepening over a four-hour period. The region between Hormoz Strait to the south is influenced by warmer mid-tropospheric air, creating a mid tropospheric significant temperature gradient associated with baroclinicity primarily in the northern and central areas of the study region, which is indicative of baroclinic disturbances. The analysis of low-level temperatures at 925 hPa (surface) suggests the presence of a temperature gradient with $\sim 7^\circ\text{C}$ (8°C) difference predominantly along the northeastern boundary of the study area (figures area not shown here), further indicating active westerly weather disturbances associated with the baroclinic structure.

[Figure 5](#) displays low-level (10 m) wind vectors and relative humidity at 850 hPa during the extreme weather event at 0000Z. [Figure 5a](#) indicates the intensification of the low-level

southeasterly winds (up to ~ 10.2 m/s) from the Oman Sea and the Indian Ocean which curve anti-clockwise, resulting in a northeasterly flow (cyclonic) towards the study area. As this figure shows, the flow of north easterlies (in the north and northwest of the study area) conflicted with that of south easterlies from the southeastern regions. This can be associated with wind shear formation in the boundaries of the thunderstorm bands and active cold front and over the northern parts of the study area causing the baroclinicity structure. [Figure 5b](#) depicts low-level relative humidity at 925 hPa, where a notable anti-cyclonic wind pattern (north easterlies) flows from the central and southern regions of the study area towards southeastern Saudi Arabia. Significant low-level humidity (90%) is observed over a localized area in the northern section, attributed to moisture influx primarily from the eastern and southeastern marine areas (Oman Sea and Indian Ocean). Conversely, the remainder of the study area lacks substantial low-level moisture sources. A Skew-T diagram for November 17, 2023, at 0000Z, centered over coordinates 25.16°N and 55.29°E indicates an unstable atmospheric profile associated with a stormy weather system, with a Convective Available Potential Energy (CAPE) calculated at 1483 J. The vertical temperature profile at this location reveals a peak humidity of around 600 hPa (Figure is not presented here).

The horizontal wind vectors (a) and relative humidity (b) at 600 hPa, shown in [Figure 6](#), depict strong northwesterly winds (cyclonic curvature) originating from the Mediterranean Sea and traversing Iraq towards the central Persian Gulf. Notably, strong (highlighted in yellow) westerly and southwesterly winds, reaching a maximum of approximately

Table 2. Conversion of latitude and longitude differences to kilometers and miles.

Latitudinal Position	Latitude Degree	Longitude Degree
	Length (km/mi)	Length (km/mi)
90°	111.7/69.4	0/0
60°	111.4/69.2	55.8/34.7
30°	110.9/68.9	96.5/60.0
0°	110.60/68.7	111.32/69.2

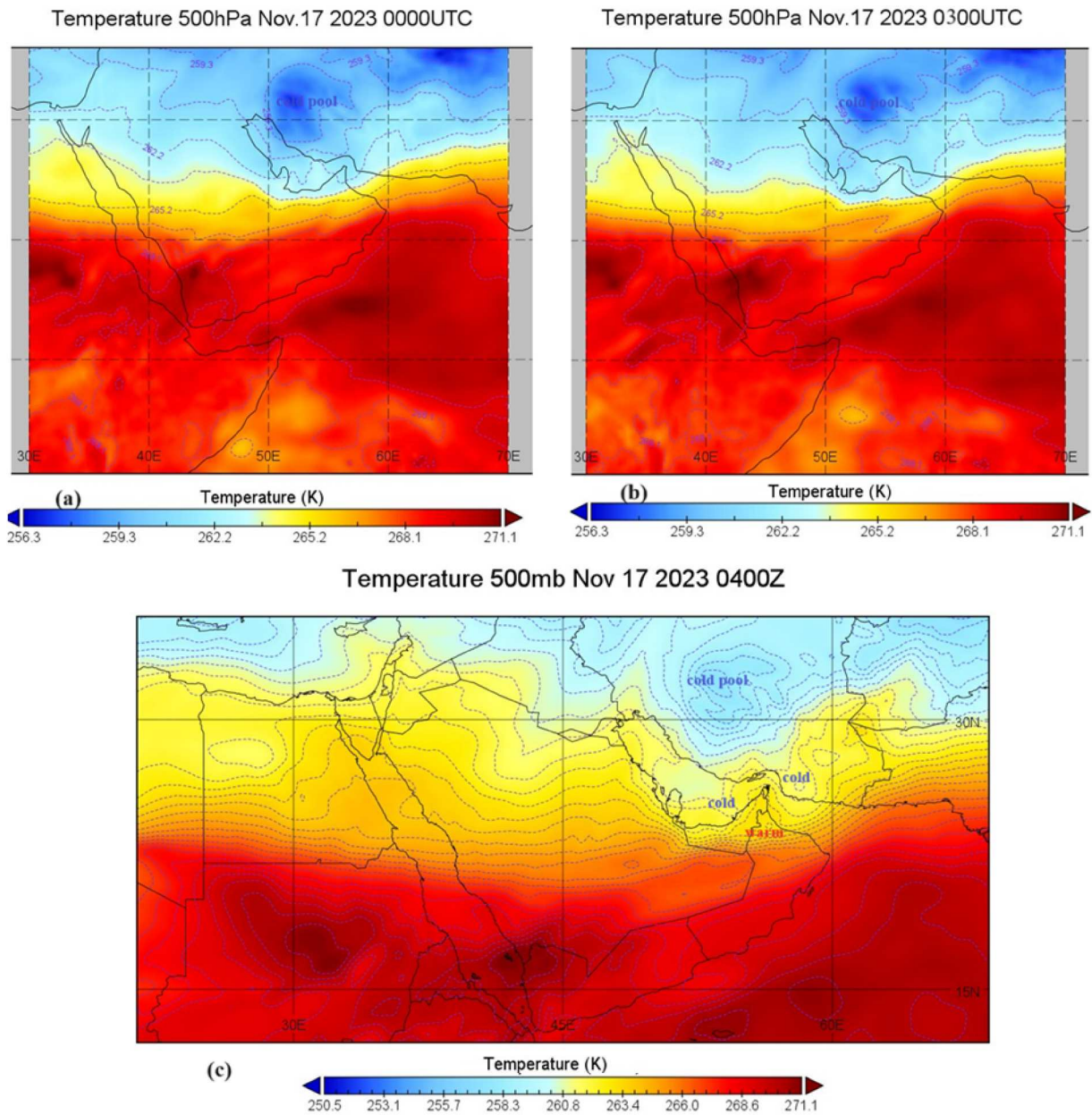


Figure 4. Hourly temperatures at 500 hPa over the study region during the extreme rainfall event on November 17, 2023, at (a) 0000Z, (b) 0003Z, and (c) 0004Z, respectively.

14 m/s, coincide with significant relative humidity levels (Figure 6b) ranging from 70-100% throughout the study area during the extreme weather event on November 17, 2023. Anomaly maps for relative humidity at 925 hPa (Figure

7a) and 600 hPa (Figure 7b) during the extreme weather day reveal increases in low and mid-level specific humidity by approximately $\sim 0.002\text{kg/kg}$ across the study area compared to long-term climatological values (1991–2020).

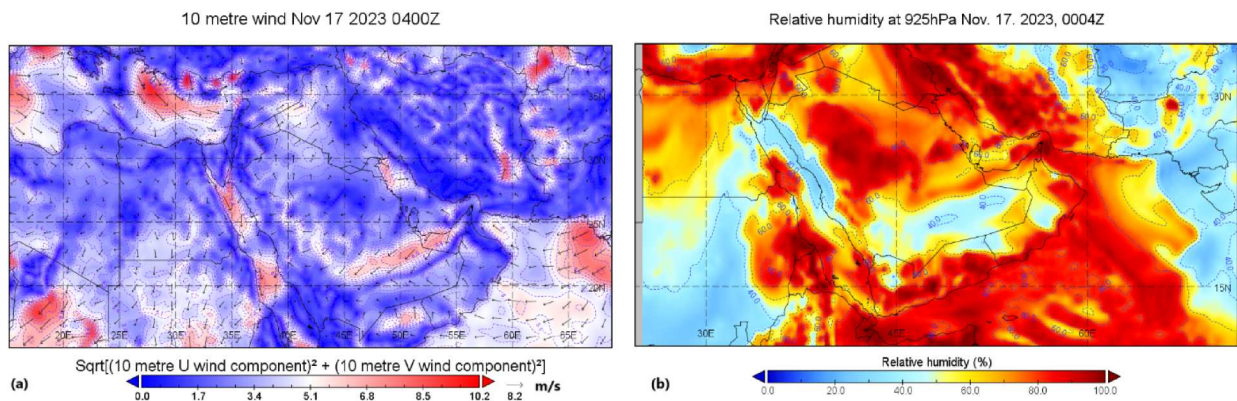


Figure 5. (a) Low-level wind vectors at 10- m level and (b) low-level relative humidity at 925 hPa on November 17, 2023, at 0400Z.

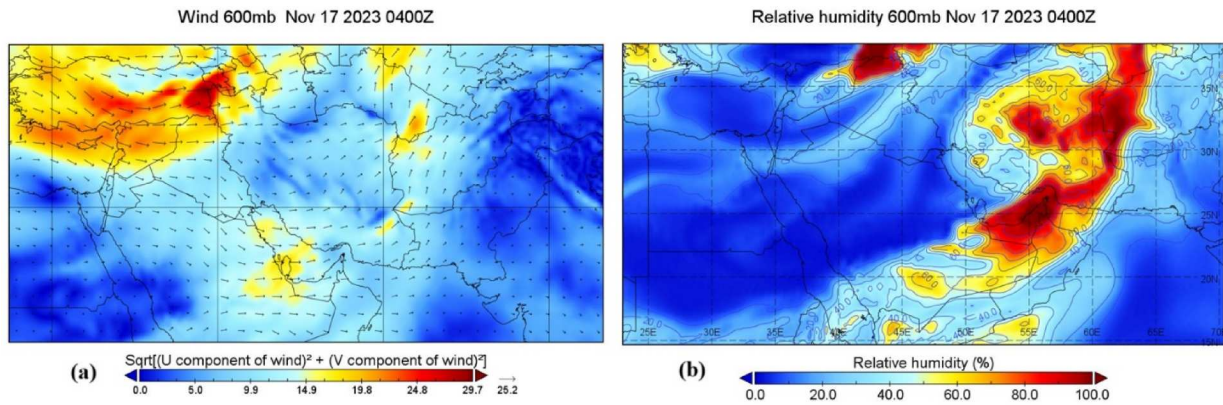


Figure 6. Horizontal structure of wind vectors (a) and relative humidity (b) at 600 hPa on November 17, 2023, at 0400Z.

Figure 8a illustrates the horizontal structure of divergence at the 200 hPa level of the jet stream over the study area at 0004Z, revealing a significant divergence center in the northern sector. This suggests the presence of upper-level cold, dry air (not shown) subsiding over the humid and warmer lower-level air, leading to instability conducive to deep convection and convective cloud formation primarily in the northern portions of the study region. Figure 8b displays relative vorticity analyzed at 500 hPa on November 17, 2023, at 0004Z, indicating a vorticity gradient producing positive vorticity advection predominantly over the southern, northern (centered over Hormoz Strait), and eastern areas (east of the 500 hPa trough), with a maximum of $2 \times 10^{-5} \text{ s}^{-1}$, juxtaposed against negative vorticity in the western parts. Positive vorticity advection enhances vertical motion and upward air movement.

Figure 9a shows a daily average map of Ertel's potential vorticity (PV) at 300 hPa on November 17, 2023, averaged over three-hour intervals from 0000Z to 2300Z, sourced from the MERRA database. This figure reveals two curved bands corresponding to a surface low-pressure system and an upper trough located to the northeast of the Black Sea (upper right corner of Figure 9a). A slight green horizontal curve extending from the Red Sea indicates a PV ($\sim 1.7 \text{ PVU}$) streamer, signifying an active westerly wave directed toward the study area. Figure 9b presents the Ertel's

potential vorticity at 300 hPa for the same date at 0400Z, derived from ERA-5 with a resolution of $0.25^\circ \times 0.25^\circ$. A prominent closed positive value of 1.5 PVU corresponds to an active westerly wave extending towards the study area. Ertel's potential vorticity plays a crucial role in modern dynamical meteorology, informing theoretical analyses, tropospheric modeling, and diagnosis of large-scale stratospheric processes (Ertel 1942, Hoskins *et al.* 1985, Holton *et al.* 1995).

Figure 10a and 10b depict wind vectors at 200 hPa for November 16 (the day preceding the extreme case) and November 17, 2023, at 0400Z, respectively. Figure 10a reveals a subtropical jet with a strong core ($\sim 50 \text{ m/s}$) centered over the Persian Gulf and west of the study area, while Figure 10b indicates a southward meander of the subtropical jet into the study area with a reduced velocity of $\sim 33.5 \text{ m/s}$. The comparison of wind vectors at 200 hPa from the previous day (0004Z) to the following day illustrates the eastward shift of the jet, positioning the cyclonic curvature over the study area during the extreme weather event. Such alterations in the waviness of both polar and subtropical jet streams can signify substantial weather fluctuations in mid-latitude regions (Martin 2021). Figure 10c presents the anomaly map for the 200 hPa wind vector during the weather system, indicating a pronounced northwesterly wind vector anomaly ($\sim 12 \text{ m/s}$) over the study area, with maximum values reaching $\sim 23 \text{ m/s}$ over Saudi Arabia. Zonal and meridional wind anomalies

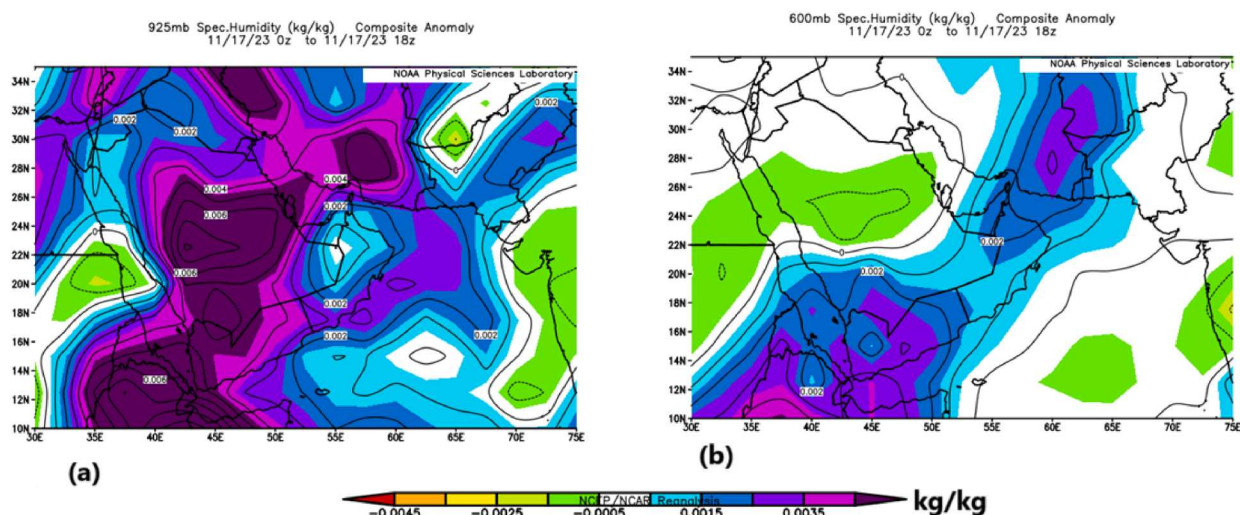


Figure 7. Anomaly maps for specific humidity at 925 hPa (a) and 600 hPa (b) on November 17 (averaged from 0000Z-1800Z), 2023, depicting departures from the 1991–2020 averages.

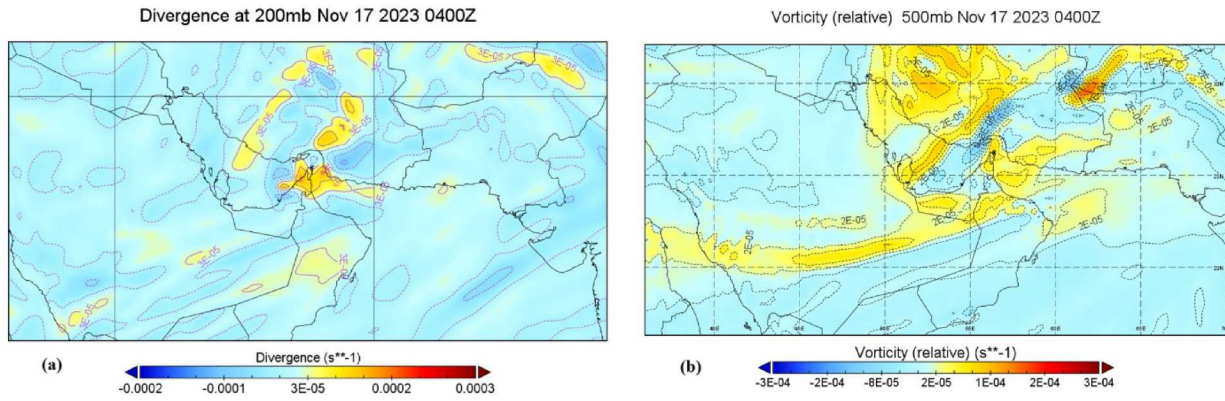


Figure 8. Divergence at 200 hPa (a) and relative vorticity at 500 hPa (b) on November 17, 2023, at 0004Z, illustrating conditions over the study area.

(not shown) further illustrate the southward shift of the subtropical jet towards lower latitudes. Notably, the weakening of zonal winds is observed predominantly over northern Iran, while significant decreases in meridional winds are recorded across Saudi Arabia, with maximum anomalies of ~ 15 m/s. This phenomenon is associated with the southward stretching of meridional winds, coupled with the penetration of upper-level cold air (500 hPa trough) into the subtropical region and the study area.

4. Conclusions

This work revealed a slight intensification of the Arabian High and the Red Sea Trough centers during the extreme event. The unique intensity of this heavy rainfall was attributed to the amplification of a mid-latitude disturbance even in middle and upper tropospheric features, produced by the Red Sea Trough, with its high relative vorticity, cold upper levels, and warm low-level temperatures. This combined with the source of moisture from two different sources, headed to severe dynamic and thermodynamic conditions favorable to an extreme heavy rainfall during a short time. The low-level wind vectors at the 850-hPa pressure level indicated the intensification of the low-level southeasterly winds (up to ~ 10.2 m/s)

from the Oman Sea and the Indian Ocean curving anti-clockwise, resulting in cyclonic flow towards the study area. This was associated with wind shear formation over the northern parts of the study area causing the baroclinicity structure in the boundaries of the cold front and thunderstorms.

The United Arab Emirates (UAE) is particularly susceptible to the impacts of climate change (Shanks 2018, Kamkar *et al.* 2022, Karkain *et al.* 2022), which threaten critical infrastructure such as energy supplies, water desalination systems, and coastal habitats along the Persian Gulf and Gulf of Oman. Projections indicate that climate change will likely exacerbate temperature, and humidity increases while reducing precipitation in the UAE (Kamkar *et al.* 2022).

The extreme weather conditions associated with rather abnormal amounts of rainfall observed during this event may be linked to broader trends in global climate change, highlighting the UAE's increasing vulnerability to such events. Also, it can be noted that by addressing potential implications such as Climate Adaptation, policymakers, and environmental managers can better prepare for the increasing frequency and intensity of extreme weather events, ensuring the UAE's long-term resilience against climate-related challenges. This can include climate adaptation strategies, such as improving infrastructure, enhancing early-warning systems, and

Time Averaged Map of Ertels potential vorticity, Instantaneous 3-hourly 0.5×0.625 deg. @300hPa
IMERRA-2 Reanalysis M2I3NPASM v5.12.41 Km2/ka/s

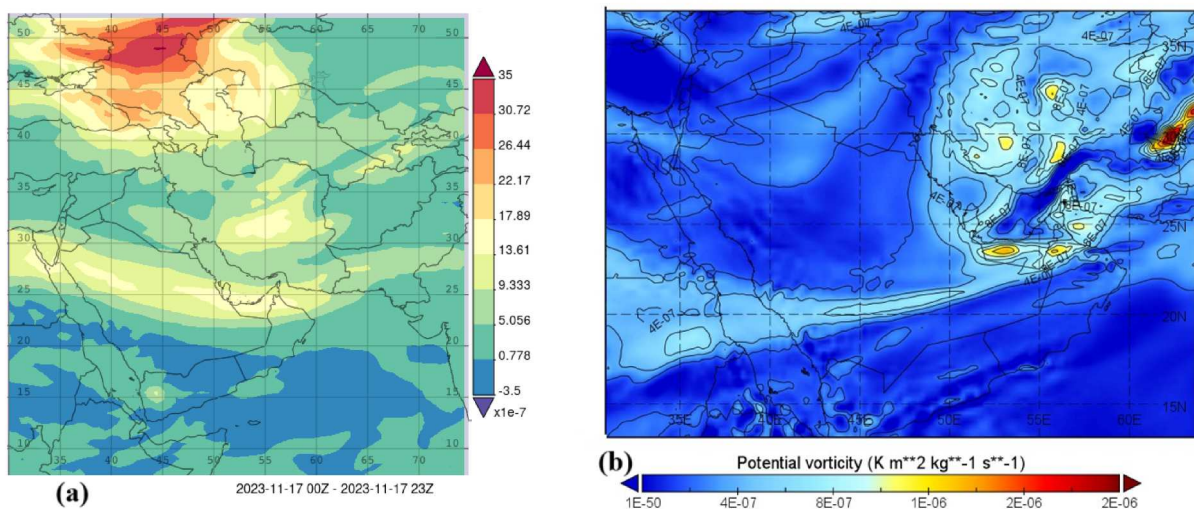


Figure 9. The Ertel potential vorticity streamer at 300 hPa for November 17, 2023, averaged every 3 h from the MERRA database (a). The same parameters depicted at 0400 UTC, sourced from the ERA-5 dataset (b).

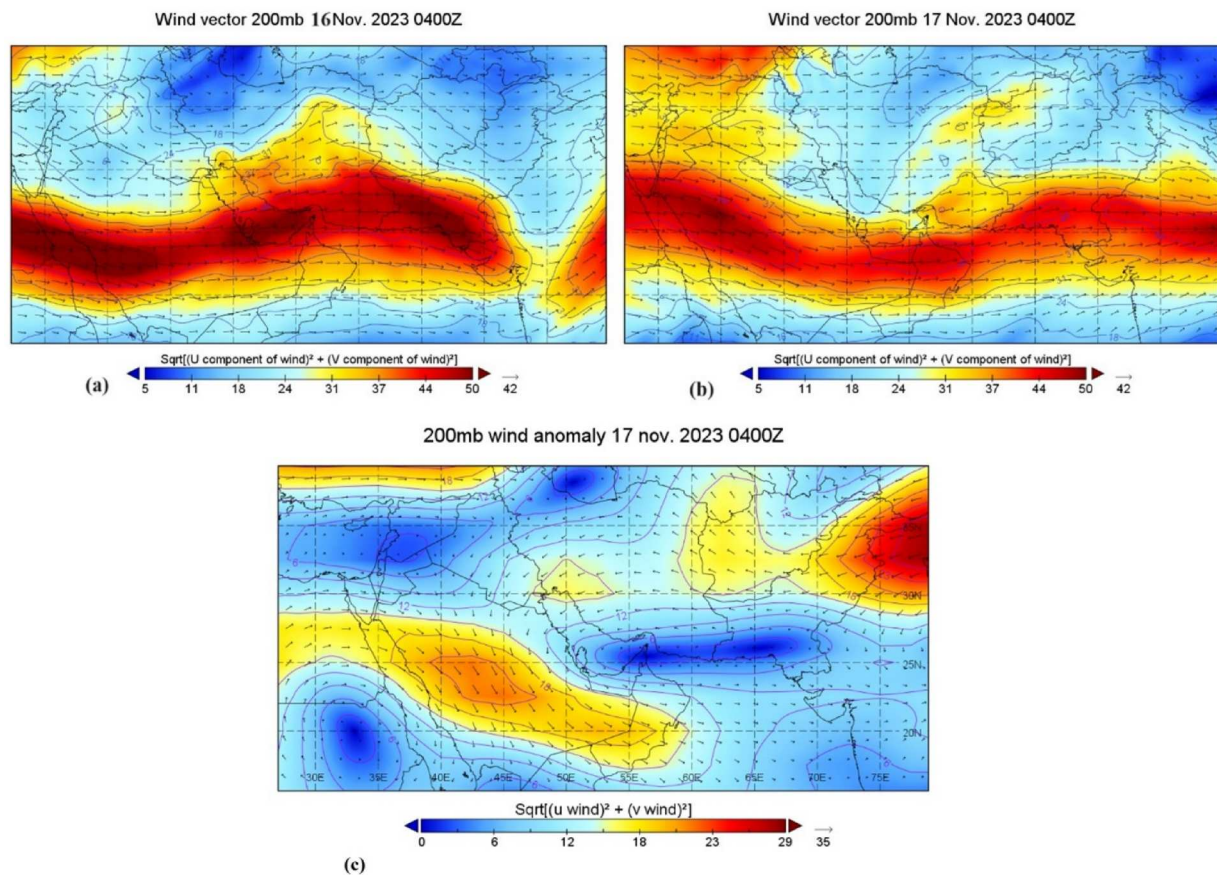


Figure 10. Wind vectors at 200 hPa for November 16, 2023 (a), and November 17, 2023, at 0400Z (b) over the study area. Anomaly map for the 200 hPa wind vector during the weather system (c).

incorporating more research to boost data collection. These efforts will help refine climate forecasting and decision-making, enabling more accurate predictions of extreme weather events. By doing so, policymakers can implement proactive measures to better protect communities, reduce damage, and ensure the UAE is prepared for the increasing frequency and intensity of extreme weather events linked to climate change.

However, the potential for extreme weather events, including rainstorms and associated flooding, remains a concern. So, considering the impact of climate change and global warming on extreme weather events in similar arid regions can point to a future with more intense and irregular rainfall patterns, leading to increased risks of flooding. These events can act as both indicators of changing climate conditions and as a basis for future predictions and adaptations. Therefore, understanding changing weather patterns in the UAE is vital for creating targeted, long-term solutions to mitigate the impacts of climate-related events.

Acknowledgements

We extend our gratitude to the European Centre for Medium-Range Weather Forecasts (ECMWF) for providing the ERA5 hourly data. We also thank the Physical Science Division, Boulder, Colorado, accessible via <http://www.esrl.noaa.gov/psd/>, as well as the Giovanni online data system developed and maintained by NASA's Goddard Earth Sciences Data and Information Services Center (GES DISC), NASA Land Processes Distributed Active Archive Center (LP DAAC) at the USGS EROS Center, and EUMETSAT for the satellite imagery archives. The authors sincerely thank the editor, associate editor, and reviewers for reviewing our manuscript and providing constructive feedback to improve our manuscript. Additionally, MR appreciates the support from Virgin Unite USA, Inc. through the Planetary Boundary Science Lab project.

Disclosure statement

No potential conflict of interest was reported by the author(s).

Notes on contributors

Farahnaz Fazel-Rastgar is a research meteorologist with a BSc in Applied Physics, an MSc in Meteorology, and a PhD in Earth and Space Science. With over ten years of experience at Iran's Meteorological Organization, she specializes in planetary atmospheric data analysis and modeling. She has also held academic roles as a Research and Teaching Assistant at York University and an Honorary Research Associate at the University of KwaZulu-Natal.

Masoud Rostami is a senior scientist at the Potsdam Institute for Climate Impact Research (PIK). He earned his PhD from Sorbonne University and remains a visiting scientist at the Laboratoire de Météorologie Dynamique (LMD). His research focuses on Earth and planetary atmospheric dynamics, geophysical fluid dynamics, and Earth System Modeling.

Bijan Fallah is a climate scientist based in Berlin, specializing in climate modeling, data analysis, and AI-driven approaches to environmental research. He has worked with the Potsdam Institute for Climate Impact Research (PIK), the German Climate Computing Center (DKRZ), and Freie Universität Berlin, focusing on large-scale climate simulations, downscaling techniques, and parallel computing. His research integrates AI and statistical methods to analyze climate impacts and develop sustainable solutions.

Venkataraman Sivakumar is a researcher specializing in atmospheric sciences, with a focus on remote sensing (both ground and spaceborne), aerosols, clouds, and the structure and dynamics of the atmosphere. His research spans extreme weather events, climate change, and space-atmosphere interactions. Currently, Prof. Venkataraman is exploring the application of machine learning techniques to advance the analysis and understanding of atmospheric phenomena.

ORCID

Farahnaz Fazel-Rastgar  <http://orcid.org/0000-0002-3904-4313>

References

- “World Meteorological Organization Climate Normals for 1991–2020: Dubai Intl Airport” (XLSX). National oceanic and atmospheric administration. p. 1. Retrieved Sep. 2024.
- Alizadeh, Z., et al., 2021. The climatological impact of the upper-tropospheric Rossby wave propagation on the Red Sea trough in winter. *Atmospheric Research*, 250, 105368. doi:10.1016/j.atmosres.2020.105368.
- Almazroui, M., 2011. Sensitivity of a regional climate model on the simulation of high intensity rainfall events over the Arabian Peninsula and around Jeddah (Saudi Arabia). *Theoretical and Applied Climatology*, 104, 261–276.
- Ashbel, D., 1938. Great floods in Sinai Peninsula, Palestine, Syria and the Syrian desert, and the influence of the Red Sea on their formation. *Quarterly Journal of the Royal Meteorological Society*, 64 (277), 635–639.
- Awad, A.M., and Almazroui, M., 2016. Climatology of the winter Red Sea trough. *Atmospheric Research*, 182, 20–29. doi:10.1016/j.atmosres.2016.07.019.
- Dayan, U., et al., 2001. A severe autumn storm over the middle-east: synoptic and mesoscale convection analysis. *Theoretical and Applied Climatology*, 69 (1–2), 103–122. doi:10.1007/s007040170038.
- De Vries, A.J., et al., 2013. Extreme precipitation events in the Middle East: dynamics of the active Red Sea trough. *Journal of Geophysical Research: Atmospheres*, 118 (13), 7087–7108. doi:10.1002/jgrd.50569.
- Didovets, I., et al., 2024. Attribution of current trends in streamflow to climate change for 12 Central Asian catchments. *Climatic Change*, 177, 1. doi:10.1007/s10584-023-03673-3.
- El-Fandy, M.G., 1948. The effect of the Sudan monsoon low on the development of thundery conditions in Egypt, Palestine and Syria. *Quarterly Journal of the Royal Meteorological Society*, 74 (319), 31–38.
- El-Fandy, M.G., 1950. Effects of topography and other factors on the movement of lows in the Middle East and Sudan. *Bulletin of the American Meteorological Society*, 31 (10), 375–381.
- Elsayed, M., et al., 2021. 2021 impact of weather extremes on wheat production in Egypt. *Middle East Journal of Agriculture Research*. doi:10.36632/mejar/2021.10.4.85.
- Ertel, H., 1942. Ein neuer hydrodynamischer Erhaltungssatz. *Die Naturwissenschaften*, 30 (36), 543–544. doi:10.1007/bf01475602.
- Esmaeili, Z., Nasr-Esfahani, M.A., and Ghadim, S.E., 2022. The role of the Red Sea in moisture feeding of flood events of Iran with emphasis on atmospheric river concept. *Meteorology and Atmospheric Physics*, 134 (3), doi:10.1007/s00703-022-00865-x.
- Fallah, B., et al., 2023. Anthropogenic influence on extreme temperature and precipitation in Central Asia. *Scientific Reports*, 13 (1). doi:10.1038/s41598-023-33921-6.
- Fallah, B., et al., 2024. Climate change impacts on Central Asia: trends, extremes and future projections. *International Journal of Climatology*.
- Fallah, B., and Rostami, M., 2024. Exploring the impact of the recent global warming on extreme weather events in Central Asia using the counterfactual climate data ATTRICI v1.1. *Climatic Change*, 177 (5), 80.
- Fazel-Rastgar, F., 2020. Extreme weather events related to climate change: widespread flooding in Iran, March–April 2019. *SN Applied Sciences*, 2 (12), doi:10.1007/s42452-020-03964-9.
- Fazel-Rastgar, F. and Sivakumar, V., 2023. A case study of an extreme flooding episode in Charikar, eastern Afghanistan. *Journal of Water and Climate Change*, 14 (12), 4689–4707. doi:10.2166/wcc.2023.462.
- Fink, A.H. and Knippertz, P., 2003. An extreme precipitation event in southern Morocco in spring 2002 and some hydrological implications. *Weather*, 58 (10), 377–387.
- Hersbach, H., et al., 2020. The ERA5 global reanalysis: Achieving a detailed record of the climate and weather for the past 70 years. doi:10.5194/egusphere-egu2020-10375.
- Holton, J.R., et al., 1995. Stratosphere-troposphere exchange. *Reviews of Geophysics*, 33 (4), 403–439. doi:10.1029/95rg02097.
- Hoskins, B.J., McIntyre, M.E., and Robertson, A.W., 1985. On the use and significance of isentropic potential vorticity maps. *Quarterly Journal of the Royal Meteorological Society*, 111 (470), 877–946. doi:10.1002/qj.49711147002.
- Insua-Costa, D., et al., 2022. A global perspective on western Mediterranean precipitation extremes. *NPJ Climate and Atmospheric Science*, 5 (1), doi:10.1038/s41612-022-00234-w.
- Itzigsohn, D., 1995. Dynamical and climatological analysis of interactions between the tropics and mid-latitudes in the Red Sea area, MSc Thesis, Department of Geophysics and Planetary Sciences, Tel Aviv University (in Hebrew), 137 pp.
- Kadhun, J.H., Al-Zuhairi, M.F., and Hashim, A.A., 2022. Synoptic and dynamic analysis of few extreme rainfall events in Iraq. *Modeling Earth Systems and Environment*, 8 (4), 4939–4952. doi:10.1007/s40808-022-01419-1.
- Kahana, R., et al., 2002. Synoptic climatology of major floods in the Negev desert. *Israel. International Journal of Climatology*, 22 (7), 867–882. doi:10.1002/joc.766.
- Kalnay, E., et al., 1996. The NCEP/NCAR 40-year reanalysis project. *Bulletin of the American Meteorological Society*, 77 (3), 437–471. doi:10.1175/1520-0477(1996)077<0437:tnyrp>2.0.co;2.
- Kamkar, F., et al., 2022. Assessing climate change indicators in the United Arab Emirates. *International Journal of Global Warming*, 26 (3), 247. doi:10.1504/ijgw.2022.121226.
- Karkain, R.M., et al., 2022. Assessing climate change indicators in the United Arab Emirates. *International Journal of Global Warming*, 26 (3), 247. doi:10.1504/ijgw.2022.10045418.
- Kistler, R., et al., 2001. The NCEP–NCAR 50-year reanalysis: monthly means CD-ROM and documentation. *Bulletin of the American Meteorological Society*, 82 (2), 247–267. doi:10.1175/1520-0477(2001)082<0247:tnnym>2.3.co;2.
- Krichak, S. O., Alpert, P., and Krishnamurti, T.N., 1997a. Interaction of topography and tropospheric flow – a possible generator for the Red Sea Trough? *Meteorol. Atmos. Phys.*, 63 (3–4), 149–158.
- Krichak, S.O., Alpert, P., and Krishnamurti, T.N., 1997b. Red Sea Trough/cyclone development – numerical investigation. *Meteorol. Atmos. Phys.*, 63 (3–4), 159–169.
- Llasat, M.C., et al., 2010. High-impact floods and flash floods in Mediterranean countries: The FLASH preliminary database. *Advances in Geosciences*, 23, 47–55. doi:10.5194/adgeo-23-47-2010.
- Martin, J. E., 2021. Recent trends in the waviness of the northern hemisphere wintertime polar and subtropical jets. *Journal of Geophysical Research: Atmospheres*, 126 (9), doi:10.1029/2020jd033668.
- Moawad, M. B., 2012. Predicting and analyzing flash floods of ungauged small-scale drainage basins in the eastern desert of Egypt. *Journal of Geomatics*, 6 (1), 23–30.
- Mohammadi, Z., Lashkari, H., and Mohammadi, M.S., 2021. Synoptic analysis and core situations of Arabian anticyclone in shortest period precipitation in the south and Southwest of Iran. *Arabian Journal of Geosciences*, 14 (12), doi:10.1007/s12517-021-07572-8.
- Ouarda, T., et al., 2014. Evolution of the rainfall regime in the United Arab Emirates. *Journal of Hydrology*, 514, 258–270. doi:10.1016/j.jhydrol.2014.04.032.
- Peel, M.C., Finlayson, B.L., and McMahon, T.A., 2007. Updated world map of the Köppen–Geiger climate classification. *Hydrology and Earth System Sciences*, 11 (5), 1633–1644. doi:10.5194/hess-11-1633-2007.
- Rienecker, M.M., et al., 2011. MERRA: NASA’s modern-era retrospective analysis for research and applications. *Journal of Climate*, 24 (14), 3624–3648. doi:10.1175/jcli-d-11-00015.1.
- Rousta, I., et al., 2016. Analysis of extreme precipitation events over central plateau of Iran. *American Journal of Climate Change*, 05 (03), 297–313. doi:10.4236/ajcc.2016.53024.
- Shanks, K., 2018. Energy performance resilience of UAE buildings to climate change. *International Journal of Environment and Sustainability*, 7, 1. doi:10.24102/ijes.v7i1.905.
- Tsvieli, Y., and Zangvil, A., 2005. Synoptic climatological analysis of ‘wet’ and ‘dry’ Red Sea troughs over Israel. *International Journal of Climatology*, 25 (15), 1997–2015. doi:10.1002/joc.1232.
- Tsvieli, Y. and Zangvil, A., 2007. Synoptic climatological analysis of Red Sea trough and non-red sea trough rain situations over Israel. *Advances in Geosciences*, 12, 137–143. doi:10.5194/adgeo-12-137-2007.
- Yu, Y., et al., 2016. Climatology of summer Shamal wind in the Middle East. *Journal of Geophysical Research: Atmospheres*, 121 (1), 289–305. doi:10.1002/2015jd024063.
- Ziv, B., et al., 2022. Identification and classification of the wet Red Sea trough over Israel. *International Journal of Climatology*, 42 (16), 10062–10082. doi:10.1002/joc.7884.